Probing coherence and noise tolerance in discrete-time quantum walks: Unveiling self-focusing and breathing dynamics

A. R. C. Buarque and W. S. Dias
Instituto de Física, Universidade Federal de Alagoas, 57072-900 Maceió, Alagoas, Brazil

(Received 28 October 2020; accepted 30 March 2021; published 16 April 2021)

The sensitivity of quantum systems to external disturbances is a fundamental problem for the implementation of functional quantum devices, quantum information, and computation. Based on remarkable experimental progress in optics and ultracold gases, we study the consequences of a short-time (instantaneous) noise while an intensity-dependent phase acquisition is associated with a qubit propagating on an N cycle. By employing quantum coherence measures, we report emerging unstable regimes in which quantum walks arise, such as self-focusing and breathing dynamics. Our numerical and analytical results unveil appropriate settings which favor the stable regime, with the asymptotic distribution surviving for weak nonlinearities and disappearing in the thermodynamic limit with $1/N$. The diagram showing the threshold between different regimes reveals the quantum gates close to Pauli-Z as more noise tolerant. As we move towards the Pauli-X quantum gate, such aptness dramatically decreases and the threshold to the self-focusing regime becomes almost unavoidable. Quantum gates close to Hadamard exhibit an unusual aspect, in which an increment of the nonlinear strength can remove the dynamics from the self-focusing regime.

DOI: 10.1103/PhysRevA.103.042213

I. INTRODUCTION

Quantum walks on a lattice have been indicated as a powerful environment for developing quantum algorithms, as well as a versatile and intuitive framework capable of performing any quantum computation [1–3]. In addition, quantum walks have been shown to be ideal testbeds for studying and exploring quantum systems [4–6]. Thus, designing and controlling such quantum processes for the long-time dynamics is a fundamental issue that requires a deep understanding.

Quantum noises are the main obstacle for performance improvement of quantum computing, since their presence can destroy a fundamental component: the delicate quantum state of qubits [7–12]. Decoherence is a physical phenomenon that typically arises from the interaction of quantum systems and their environment. In discrete-time quantum walks (DTQWs), the decoherence in the quantum gates drives the walker to a spreading rate quadratically slower in the long-time limit [13–15]. Broken links, simultaneous measurements of chirality and position, random phases, and fluctuations in a given preestablished unitary operation can also induce the same behavior [16–19]. Such results have been corroborated by experimental studies that describe the decoherence inducing a crossover of quantum dynamics from ballistic to diffusive [20–22]. Sub-ballistic and Anderson localized regimes have been reported for quantum walks with specific irregularities [23–25]. Effects of decoherence on discrete-time quantum walks have been associated with a very fast mixing time and uniform distribution regardless of the initial state of the system and the parity of lattice size [26–31].

Nonlinear phenomena on a DTQW have also been investigated, in which its source emerges from different frameworks [32–38]. An anomalous slow diffusion has been reported for feed-forward DTQWs, a nonlinear quantum walk in which the coin operator depends on the coin states of the nearest-neighbor sites [32]. Feed-forward DTQWs have provided the dynamics of a nonlinear Dirac particle, with a description of solitonic behavior and the collisional phenomena between them [33]. A modified conditional shift operator displaying a dependence on the local occupation probability shows solitonlike propagation and a chaotic regime [34]. By using DTQWs which combine zero modes with a particle-conserving nonlinear relaxation mechanism, a conversion of two zero modes of opposite chirality into an attractor-repeller pair of nonlinear dynamics was reported [36]. One of the earliest studies reporting the emergent nonlinear phenomena on DTQWs studied the nonlinear self-phase modulation on the wave function during the walker evolution [37]. Restricted only to Hadamard quantum gates, nondispersive pulses and chaoticlike dynamics have been reported. A detailed study exploring other quantum gates reveals a rich set of dynamical profiles, including the self-trapped quantum walks, a localized regime in which the quantum walker remains localized around its initial position [38]. An interesting mathematical treatment on nonlinear DTQWs is described in Ref. [35].

Although it seems natural to consider linearity in the quantum regime, quantum-mechanical systems the effective evolution of which is governed by a nonlinear dynamics have been described in both optics [39] and Bose-Einstein condensates [40,41], the same environments where quantum walks have shown a remarkable experimental progress [6,20–22,42,43]. By considering that fault-tolerant architectures are built from the understanding of each possible ingredient, acting simultaneously or not, we studied here the weight of a

noise on the dynamics of a quantum walker within a nonlinear framework. We consider a small and instantaneous amount of decoherence on the qubit distribution, which expresses a measurement process or other environmental intervention. Nonlinear character is associated with an intensity-dependent phase acquisition with a qubit propagating on the lattice, which can represent an emerging third-order nonlinear susceptibility at photonic setups or interatomic interactions in ultracold atomic systems. By systematically exploring quantum coherence measures, we report appropriate settings which favor the stable regime. However, unstable regimes unveil DTQWs never once attained, such as the self-focusing and breathing dynamics. The stability threshold was investigated by varying the quantum gates, as well as the lattice size, which estimates the quantum behavior in the thermodynamic limit.

II. MODEL

Here, we consider an intensity-dependent (nonlinear) phase acquisition associated with a quantum walker propagating on a one-dimensional lattice of interconnected sites [37,38]. More precisely, the walker consists of a qubit, the state $|\psi\rangle$ of which is associated with its position and internal state (chirality), which can be described by spin or polarization states. Thus, $|\psi\rangle$ belongs to a Hilbert space $H = H_c \otimes H_p$, with positions described by the orthonormal basis $\{|n\rangle\colon n \in \mathbb{Z}\}$ spanning the position Hilbert space H_p, while the internal state is associated with a two-dimensional Hilbert space H_c spanned by an orthonormal basis $\{|R\rangle = (1,0)^T, |L\rangle = (0,1)^T\}$.

Each step of evolution consists in quantum gates $\hat{C}$ located in the lattice sites which act on the quantum walker and shuffles its internal state, followed by spatial shifts to adjacent sites (left or right) according to its new chirality. Thus, given a general state written as

$$|\psi(t)\rangle = \sum_n [a_{n,t}|R\rangle + b_{n,t}|L\rangle] \otimes |n\rangle, \tag{1}$$

in which amplitudes $a_{n,t}$ and $b_{n,t}$ are complex numbers that satisfy $\sum_n (|a_{n,t}|^2 + |b_{n,t}|^2) = 1$, a single step of dynamical evolution is performed by applying the unitary transformation $|\psi(t+1)\rangle = \hat{U}|\psi(t)\rangle$.

The standard (linear) protocol regards $\hat{U} = \hat{S}(\hat{C} \otimes I_p)$. I_p describes the identity operator in space of positions and $\hat{C}$ is an arbitrary $SU(2)$ unitary operator given by

$$\begin{aligned}\hat{C} = {} & \cos(\theta)|R\rangle\langle R| - \sin(\theta)|R\rangle\langle L| \\ & + \sin(\theta)|L\rangle\langle R| + \cos(\theta)|L\rangle\langle L|,\end{aligned} \tag{2}$$

in which the parameter $\theta \in [0, 2\pi]$ controls the variance of the probability distribution of the walk. The conditional shift operator $\hat{S}$ then performs $\hat{S}(|R\rangle \otimes |n\rangle) = |R\rangle \otimes |n+1\rangle$ and $\hat{S}(|L\rangle \otimes |n\rangle) = |L\rangle \otimes |n-1\rangle$.

In our quantum algorithm, the qubit acquires an intensity-dependent (nonlinear) phase in each step of the previous protocol. We consider a quadratic nonlinearity depending on the chirality state, which can represent either nonlinear optical media in photonic setups or the interactions between atoms for ultracold atomic systems. Thus, we add to dynamical evolution protocol ($\hat{U}$) one more operator

$$\begin{aligned}\hat{K}^t = {} & \sum_n (e^{i2\pi\chi|\psi^t_{n,R}|^2}|R\rangle\langle R| \\ & + e^{i2\pi\chi|\psi^t_{n,L}|^2}|L\rangle\langle L|) \otimes |n\rangle\langle n|,\end{aligned} \tag{3}$$

such that $\hat{U}(t) = \hat{S}(\hat{C} \otimes I_p)\hat{K}^{t-1}$. The parameter χ denotes the nonlinear strength of the medium and $\chi = 0$ restores the standard (linear) protocol. Furthermore, periodic boundary conditions are assumed on the conditional shift operator

$$\begin{aligned}\hat{S} = {} & \sum_{n=1}^{N-1} |n+1\rangle\langle n| \otimes |R\rangle\langle R| + \sum_{n=2}^{N} |n-1\rangle\langle n| \otimes |L\rangle\langle L| \\ & + |1\rangle\langle N| \otimes |R\rangle\langle R| + |N\rangle\langle 1| \otimes |L\rangle\langle L|,\end{aligned} \tag{4}$$

in order to describe the N-cycle architecture employed here. The important framework of DTQWs on cycles has been used to display how quantum algorithms can be quadratically faster than its classical correspondent [2] and how decoherence can be useful in quantum walks [26], for example. Rigorous treatment for noiseless DTQWs on N cycles has proved the long-time average probability distribution of finding the qubit in each site as being uniform on the sites for odd N and nonuniform for even N [2,44]. Thus, we assume odd-N lattices with the initial state of a qubit given by

$$|\psi(0)\rangle = \frac{1}{\sqrt{2N}} \sum_{n=1}^{N} (|R\rangle + i|L\rangle) \otimes |n\rangle, \tag{5}$$

superposed to a weak noise ($\epsilon = 10^{-3}/\sqrt{2N}$). The latter expresses the interaction with environment, which can represent a measurement process. Hence, we evolve the state of a quantum walker the initial amplitudes of which at each site are randomly distributed in the interval $[\frac{1}{\sqrt{2N}} - \epsilon, \frac{1}{\sqrt{2N}} + \epsilon]$, in which a proper normalization is employed to ensure the unitary norm of the resulting distribution.

III. RESULTS

We start following the dynamical evolution protocol described above and computing the quantum coherence, the rigorous measurement framework of which has only been developed recently [45,46]. Among the advisable measures, we compute the $l1$ norm coherence

$$\mathcal{C}_{l1}(t) = \sum_i \sum_{i' \neq i} |\rho_{i,i'}(t)|, \tag{6}$$

defined as a sum of the absolute values of all off-diagonal elements in the density matrix $\rho = |\psi(t)\rangle\langle\psi(t)|$ under the reference basis. By considering the experimental character an important issue, we observe such quantity being employed to directly measure quantum coherence of an unknown quantum state [47]. Starting from an initial state maximally coherent [Eq. (5)] [45,46], we show in Fig. 1 the $l1$ norm coherence of the whole system at each time step for lattices with $N = 101$ sites ruled by quantum gates Hadamard ($\theta = \pi/4$) [Figs. 1(a)–1(d)] and $\theta = \pi/3$ [Figs. 1(e)–1(h)] homogeneously distributed. In absence of nonlinearity ($\chi = 0.00$) both quantum gates induce a dynamics with fluctuations over time around a saturation value ($\mathcal{C}_{l1}(t) \sim 2N$), which are

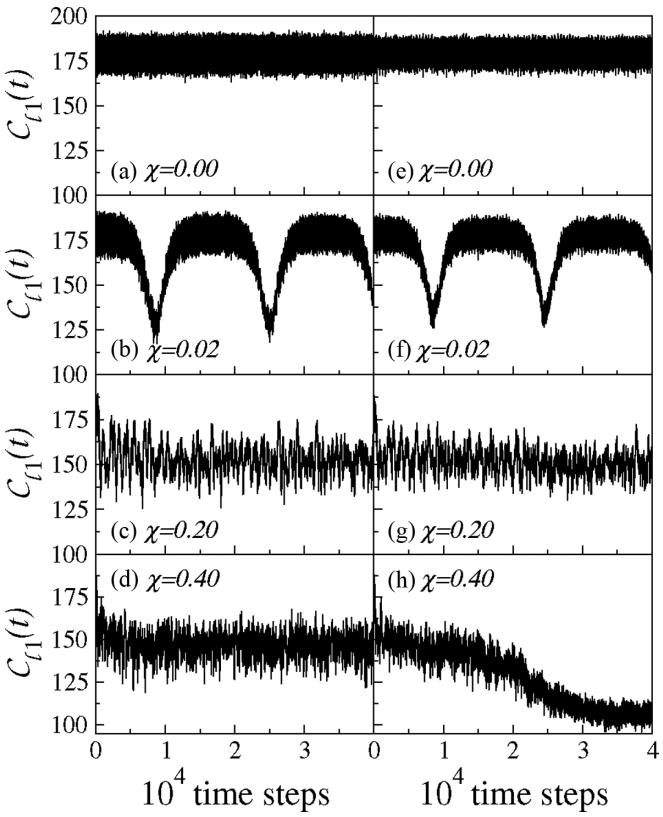

FIG. 1. Time evolution of the l_1 norm coherence of the whole system for lattices with $N = 101$ sites and ruled by quantum gates (a)–(d) $\theta = \pi/4$ and (e)–(h) $\theta = \pi/3$ homogeneously distributed. Oscillatory patterns suggest the lack of stability of the stationary distribution as the nonlinear parameter χ increases, with the emergence of regular and irregular (chaoticlike) breathing dynamics. Above a critical nonlinear strength, which seems to depend on the quantum gate, the further decrease in quantum coherence after some transient time indicates the wave packet becoming even narrower.

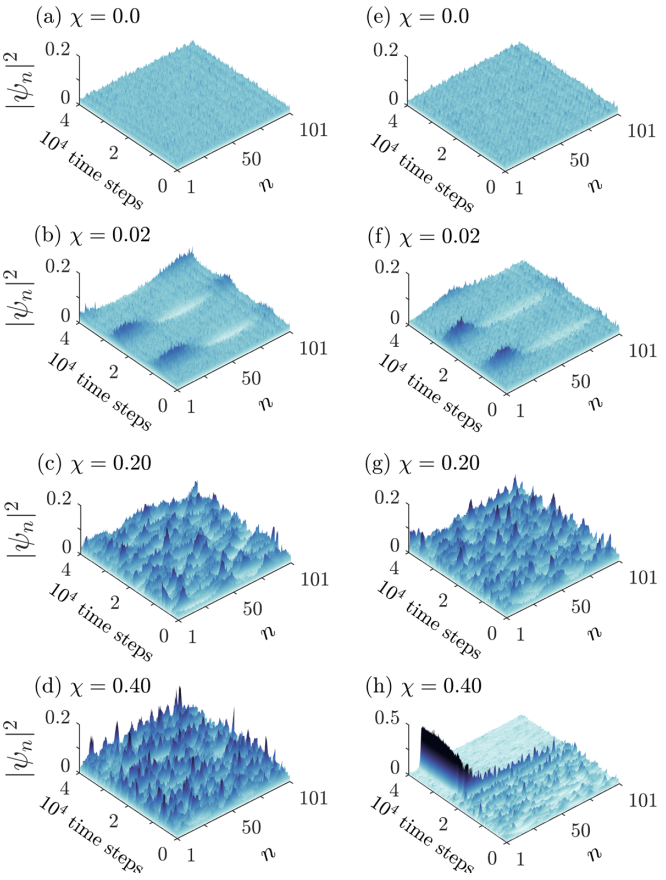

FIG. 2. Time evolution of the density of probability in position space of a quantum walker for the same configurations of θ and χ used in Fig. 1: (a)–(d) $\theta = \pi/4$ and (e)–(h) $\theta = \pi/3$. Corroborating the previous results, we observe clear signatures of regular breathing dynamics for weak nonlinearities. Although both scenarios culminate in a chaoticlike regime as the nonlinear parameter (χ) increases, the self-focusing quantum walk emerges only for $\theta = \pi/3$, which suggests a phenomenology with quantum gate dependence.

fully consistent with previous literature [46]. However, this behavior is heavily modified as χ grows. In Figs. 1(b) and 1(f), we observe the quantum coherence losing stability and developing regular breaths for a small amount of nonlinearity ($\chi = 0.02$). As we further increase the nonlinearity, breathing dynamics gives way to fluctuations the average value of which is decreased when compared to the linear regime. Such fluctuations become more rough, suggesting a chaotic aspect. However, both lattices exhibit different behaviors as χ increases even more. Lattices governed by Hadamard quantum gates remain with coherence exhibiting rough fluctuations around a decreased saturation value ($\mathcal{C}_{l1}(t) \sim 3N/2$), just as $\chi = 0.20$. On the other hand, the coherence for lattices ruled by $\theta = \pi/3$ quantum gates reveals an additional decrease after an initial transient, with oscillations $\mathcal{C}_{l1}(t) \sim N$ [see Figs. 1(d) and 1(h)].

Since fluctuations in quantum coherence are related to the oscillatory nature of the probability distribution [26], we investigate the probability density distribution $|\psi_n(t)|^2$. We use in Fig. 2 the same configurations shown in Fig. 1, with Figs. 2(a)–2(d) and Figs. 2(e)–2(f) illustrating the dynamical behaviors for lattices governed by $\theta = \pi/4$ and $\pi/3$ quantum gates, respectively. Corroborating the coherence measures, the spreading of the qubit remains uniformly extended over the entire lattice while $\chi = 0.0$, which signals the stability of the uniform distribution even after the disturbance. Such stability may disappear when nonlinearity is present, giving way to different regimes. Fully agreeing with the expectations created from the coherence measures, the wave packet develops regular breathings for very small nonlinearities and irregular breathings, with a chaoticlike aspect, for strong enough nonlinearities. The similarity between both lattices vanishes with $\chi = 0.40$. A self-focusing regime emerging after an initial transient clarifies the strong decreasing of the coherence reported for lattices with $\theta = \pi/3$.

In order to better understand, we follow the time evolution for a long time looking for χ configurations able to remove the qubit dynamics from the limiting distribution. In Fig. 3 we show the relationship between the quantum gates (θ) and the critical nonlinearity (χ_{sd}), above which the distribution becomes unstable. We observe the stationary regime surviving to a greater range of nonlinearities when the system is managed by quantum gates close to Pauli-Z ($\theta = 0$). On the

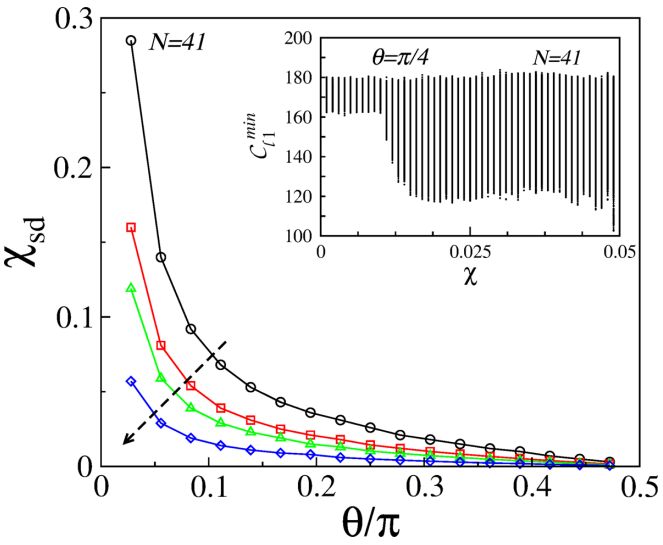

FIG. 3. Critical nonlinearity of the stationary state (χ_{sd}) as a function of θ (π units) showing quantum gates close to Pauli-Z better able to sustain the stationary regime. A monotonic decreasing of χ_{sd} as we move θ towards the Pauli-X gate is also observed, regardless of the size N (arrow points to the growth of N). Inset: All the minima of the coherence ($\mathcal{C}_{l1}^{\min}$) as a function of the nonlinear strength (χ) illustrating the critical point χ_{sd}, signaled by the significant change in width of $\mathcal{C}_{l1}^{\min}$, which comes from the lack of stability and the emerging breathing dynamics.

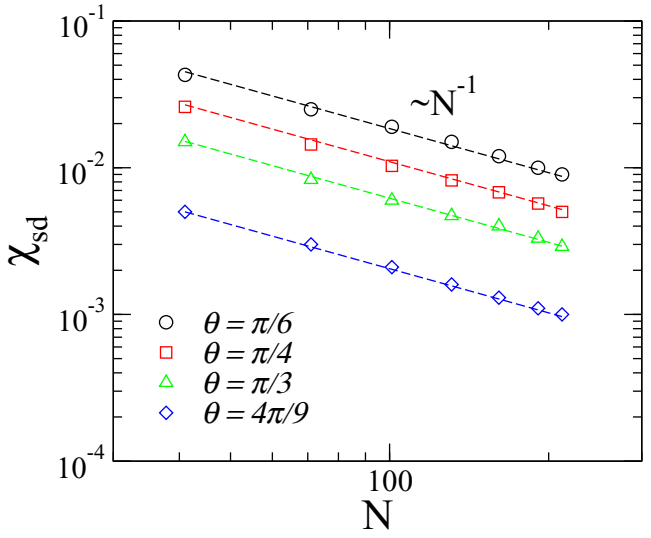

FIG. 4. Critical nonlinearity of the stationary state (χ_{sd}) computed for different lattice sizes and some representative quantum gates. The χ_{sd} vs N analysis confirms the size dependence of the critical nonlinearities and reveals a gate-independent scaling $\chi_{sd} \propto 1/N$, which indicates the requirement for error-free operations to preserve the stable regime in the thermodynamic limit $N \to \infty$.

other hand, systems governed by quantum gates nearby to Pauli-X ($\theta = \pi/2$) are more sensitive, with minor critical nonlinearities. Thus, quantum gates close to Pauli-Z are less liable to provide qubits with logical errors. The stationary regime threshold exhibits a monotonic decreasing as we move towards the Pauli-X quantum gates. Such scenario clearly demonstrates the sensitivity associated with the interference terms of the quantum gates, which has its influence amplified by the nonlinear component. The figure also shows a relationship between the critical nonlinearity and the size N, with the arrow pointing to the growth of N. The monotonic decline of χ_{sd} as we leave systems ruled by Pauli-Z towards Pauli-X systems remains unchanged. However, the increase of lattice size makes the system more susceptible to instability, since the range of nonlinearities capable of sustaining the stationary regime decreases. The inset illustrates the critical point χ_{sd}, above which the distribution becomes unstable. We recorded all the minima of $l1$ norm coherence ($\mathcal{C}_{l1}^{\min}$) for every time step throughout the dynamic evolution of a system ruled by Hadamard quantum gates. By plotting $\mathcal{C}_{l1}^{\min}$ as a function of the nonlinear strength χ, we observe a well-defined change in width of $\mathcal{C}_{l1}^{\min}$ which is consistent with the lack of stability and the emerging breathing dynamics [see Figs. 1(a), 1(b) 1(e), and 1(f)].

The dependence between the critical nonlinearity and the lattice size, which is suggested in Fig. 3, is shown for some representative quantum gates in Fig. 4. The χ_{sd} vs N analysis exhibits the critical nonlinearity scaling with $1/N$, regardless of employed quantum gates. This behavior indicates the stationary regime disappearing with $N \to \infty$ for any finite nonlinear strength, i.e., the stationary regime requires systems with error-free operations in the thermodynamic limit. Such feature can be analytically reached by using the connection between the dynamics of the discrete-time quantum walkers and the Dirac particles. In absence of noise, previous studies have shown a massive Dirac particle can be simulated on a discrete-time quantum walk, for both the linear [48–52] and nonlinear [33] systems. Interesting scenarios in which discrete-time quantum walkers exhibit behavior congruous to a massless Dirac fermion have also been reported [52–54]. Following the formalism employed in Refs. [33,51], which shortly consists in taking an effective Hamiltonian for the dynamics by defining a displacement operator using momentum $\hat{p}$ as $e^{\pm\hat{p}\Delta x}\psi(x) = \psi(x \pm \Delta x)$ and relating it to the shift operator, the discrete-time quantum walk evolution can be written analogous to the $1+1$-dimensional Dirac equation (in units of $\hbar = 1$) as

$$i\partial_t\psi = (-ic\alpha\partial_x + \beta mc^2 + \chi|\psi|^2)\psi. \tag{7}$$

The equivalent terms of mass, speed of light, and Dirac matrices are related with quantum gates and Pauli matrices. Although the familiar Dirac Hamiltonian exhibits a linear equation in momentum, terms quadratic in momentum can play an important role in characteristic scenarios, such as for the formation of topological insulators [55,56]. Here, our model also required quadratic corrections $\propto p^2$ to the Dirac equation, justified from a second-order approximation in $e^{\pm i\hat{p}}\psi(t,x)$ [33,51], which results in a modified Dirac equation as follows:

$$i\partial_t\psi = \big(-ic\alpha\partial_x + \beta mc^2\partial_x^2 + \beta mc^2 + \chi|\psi|^2\big)\psi. \tag{8}$$

By considering the parametrization of Ref. [51], the mass and speed of light equivalent terms are $m = \sin(\theta)$ and $c = 1$, respectively. x is the spatial coordinate, $\alpha = -cos(\theta)\sigma_3 +$

$\sin(\theta)\sigma_1$, and $\beta = \sigma_2$, where σ_i $(i = 1, 2, 3)$ are Pauli matrices. Note that α and β are Hermitian matrices satisfying

$$\alpha^2 = \beta^2 = \mathbb{I} \quad \text{and} \quad \alpha\beta + \beta\alpha = 0. \tag{9}$$

To perform a stability analysis of the stationary regime when subject to a perturbation, we start by observing that the continuous version of Eq. (8) supports a continuous-wave solution $\psi(t) = \psi_0 e^{-i(\beta mc^2 + \chi|\psi_0|^2)t}$, with $\psi_0 \in \mathrm{Re}$ without loss of generality. Just like in the numerical analysis, we impose a slight perturbation $\epsilon(x, t)$ in its amplitude:

$$\psi(x, t) = [\psi_0 + \epsilon(x, t)]e^{-i(\beta mc^2 + \chi|\psi_0|^2)t}. \tag{10}$$

By considering a standard linearization as a function of the initial state of the qubit $[\epsilon(x, t) \ll \psi_0]$, we obtain the following time evolution equation for the perturbation:

$$i\partial_t\epsilon = -ic\alpha\partial_x\epsilon + \beta mc^2\partial_x^2\epsilon + \chi|\psi_0|^2(\epsilon + \epsilon^*). \tag{11}$$

Here, ϵ^* denotes the complex conjugate of ϵ and the abbreviation $\epsilon = \epsilon(x, t)$ has been used. Since a white noise random perturbation exhibits a wide spectral range, which includes all harmonic contributions, we study solutions given by

$$\epsilon(x, t) = a_1 e^{i(kx - \Omega t)} + a_2 e^{-i(kx - \Omega t)}, \tag{12}$$

where a_1 and a_2 are the amplitudes of the weak modulation, k is the modulation wave number, and Ω is the frequency. Substituting Eq. (12) into Eq. (11) and considering its nontrivial solution, we obtain the dispersion relation

$$\Omega = c\alpha k \pm \sqrt{\beta mc^2 k^2(\beta mc^2 k^2 - 2\chi|\psi_0|^2)}. \tag{13}$$

This result shows the stability of the stationary regime for disturbances with large wave vectors, since Ω remains real. In contrast, $\Omega \in \mathrm{Im}$ reveals an exponential amplification of all wave vectors with $k < \sqrt{2\chi|\psi_0|^2/\beta mc^2}$, which results in breakup of continuous waves and thus describes the instability of the uniform distribution. Given the nature and the boundary conditions of the system, the allowed harmonic waves have wave numbers in the interval $2\pi/N < k < 2\pi$. Since the wave-function normalization for a uniform solution provides $\psi_0 = 1/\sqrt{N}$, we observe the characteristic nonlinear strength above which the solution is unstable as being $\chi_{sd} \propto 1/N$, in full agreement with Fig. 4.

By considering the implementation of a universal set of quantum gates as crucial for a quantum computing architecture, we extend our numerical experiments and show a χ vs θ diagram in Fig. 5. Here, we compute the long-time average of $\overline{C}_{l1}(t_\infty)$ for $N = 101$ lattice sites. Data reveal the stationary regime surviving for weaker nonlinearities, prevailing for systems configured next to the Pauli-Z quantum gate, which is characterized by leaving the basis state $|L\rangle$ unchanged and takes $|R\rangle$ to $-|R\rangle$. Although Fig. 2 suggests the stationary, breathing, chaoticlike, and self-focusing regimes in ascending order of nonlinearity, the breathing regime persists for systems with quantum gates close to Pauli-Z even for strong nonlinearities. On the other hand, systems with quantum gates nearby to Pauli-X exhibit a fairly narrow range of χ for breathing dynamics. The emergence of the chaoticlike regime is predominantly surrounding the $(\theta = \pi/6)$ quantum gates, which arises for an intermediate nonlinear strength. The self-focusing regime appears around the quantum gates

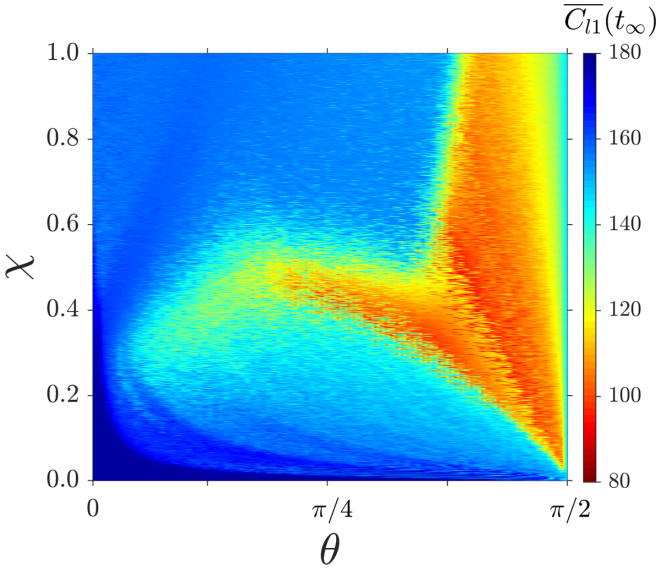

FIG. 5. Plot of χ vs θ for the long-time average of the l_1 norm coherence. Quantum gates close to Pauli-Z are more liable to sustain the stationary distribution. As we increase θ towards the Pauli-Z gate $(\theta = \pi/2)$, such propensity vanishes and different scenarios emerge as we change χ: Breathing dynamics, chaoticlike, and self-focusing quantum walks. The last ones are predominant when θ gets close to the Pauli-Z gate. An unusual aspect is reported for quantum gates close to Hadamard, in which an increment of χ can remove the dynamics from the self-focusing regime.

of Hadamard, preceded by chaoticlike, breathing, and stationary regimes in decreasing order of nonlinearity. However, we observe an unusual threshold between the self-focusing and chaoticlike regimes: The increment on the nonlinear parameter is able to direct the system from the self-focusing to the chaoticlike regime, which persists as the nonlinearity increases. Such remarkable feature agrees with report of self-trapped quantum walks described for narrow qubits spreading in noiseless systems [38]. For systems ruled by quantum gates close to Pauli-X, which is characterized by mapping $|L\rangle$ to $|R\rangle$ and $|R\rangle$ to $|L\rangle$, the self-focusing regime emerges for very weak nonlinearities and remains for the strongest nonlinearities. On the other hand, the self-focusing regime is absent as θ gets very close to Pauli-Z.

IV. CONCLUSIONS

In summary, we have implemented a quantum protocol in order to rate the sensitivity to a short-time (instantaneous) noise while nonlinear components are present in a discrete-time quantum walk. The intensity-dependent nonlinearity is based on possible third-order nonlinear susceptibility in optical setups or emergent interatomic interactions in ultracold atomic systems, while the noise can represent a measurement process or other environmental intervention. Our results unveil optimal sets of operating parameters that favor a stable operation. Quantum gates close to Pauli-Z are more noise tolerant, contrary to the behavior exhibited by quantum gates near Pauli-X gates. When it loses stability, the system may present breathing dynamics and self-focusing quantum walks.

Numerical and analytical analysis exhibits the crossover from the uniform distribution to the unstable regime decaying as $1/N$ reveals a fault-intolerant system in the thermodynamic limit ($N \to \infty$), i.e., nonlinearities may be responsible for the inability to encode and decode qubits robustly. We consider optical systems as the most promising for a current experimental achievement, in which the use of Kerr-like optical media in the optical paths of experimental settings such as linear cavities [57], optical rings [58,59], Michelson interferometers [60], and optical lattices [61] would be responsible for nonlinear character. Another possibility consists of an optical network with a cascade of beam splitters, the adjustable transmission of which would be conditioned to the output of photodetectors for each path [32]. In addition to contributing to the deeper fundamental understanding on discrete-time quantum walks, breathing and self-focusing quantum walks also bring applicability prospects for microresonators, lensinglike effects, and wave guiding, which arises from accumulated self-focusing.

ACKNOWLEDGMENTS

This work was partially supported by CAPES (Coordenação de Aperfeiçoamento de Pessoal do Nível Superior), CNPq (Conselho Nacional de Densenvolvimento Científico e Tecnológico), and FAPEAL (Fundação de Apoio à Pesquisa do Estado de Alagoas).

[1] A. M. Childs, Phys. Rev. Lett. **102**, 180501 (2009).
[2] D. Aharonov, A. Ambainis, J. Kempe, and U. Vazirani, in *Proceedings of the Thirty-Third Annual ACM Symposium on Theory of Computing* (Association for Computing Machinery, New York, 2001), pp. 50–59.
[3] A. M. Childs and J. Goldstone, Phys. Rev. A **70**, 022314 (2004).
[4] L. Xiao, K. Wang, X. Zhan, Z. Bian, K. Kawabata, M. Ueda, W. Yi, and P. Xue, Phys. Rev. Lett. **123**, 230401 (2019).
[5] R. Vieira, E. P. M. Amorim, and G. Rigolin, Phys. Rev. Lett. **111**, 180503 (2013).
[6] D. Xie, T.-S. Deng, T. Xiao, W. Gou, T. Chen, W. Yi, and B. Yan, Phys. Rev. Lett. **124**, 050502 (2020).
[7] C. H. Bennett, D. P. DiVincenzo, J. A. Smolin, and W. K. Wootters, Phys. Rev. A **54**, 3824 (1996).
[8] D. A. Lidar, I. L. Chuang, and K. B. Whaley, Phys. Rev. Lett. **81**, 2594 (1998).
[9] C. L. Degen, F. Reinhard, and P. Cappellaro, Rev. Mod. Phys. **89**, 035002 (2017).
[10] J. J. Wallman and J. Emerson, Phys. Rev. A **94**, 052325 (2016).
[11] E. T. Campbell, B. M. Terhal, and C. Vuillot, Nature (London) **549**, 172 (2017).
[12] S. J. Beale, J. J. Wallman, M. Gutiérrez, K. R. Brown, and R. Laflamme, Phys. Rev. Lett. **121**, 190501 (2018).
[13] T. A. Brun, H. A. Carteret, and A. Ambainis, Phys. Rev. Lett. **91**, 130602 (2003).
[14] T. A. Brun, H. A. Carteret, and A. Ambainis, Phys. Rev. A **67**, 032304 (2003).
[15] N. Konno, Fluct. Noise Lett. **05**, L529 (2005).
[16] D. Shapira, O. Biham, A. J. Bracken, and M. Hackett, Phys. Rev. A **68**, 062315 (2003).
[17] A. Romanelli, R. Siri, G. Abal, A. Auyuanet, and R. Donangelo, Physica A **347**, 137 (2005).
[18] A. C. Oliveira, R. Portugal, and R. Donangelo, Phys. Rev. A **74**, 012312 (2006).
[19] J. Košík, V. Bužek, and M. Hillery, Phys. Rev. A **74**, 022310 (2006).
[20] M. A. Broome, A. Fedrizzi, B. P. Lanyon, I. Kassal, A. Aspuru-Guzik, and A. G. White, Phys. Rev. Lett. **104**, 153602 (2010).
[21] A. Schreiber, K. N. Cassemiro, V. Potoček, A. Gábris, I. Jex, and C. Silberhorn, Phys. Rev. Lett. **106**, 180403 (2011).
[22] A. Regensburger, C. Bersch, B. Hinrichs, G. Onishchukov, A. Schreiber, C. Silberhorn, and U. Peschel, Phys. Rev. Lett. **107**, 233902 (2011).
[23] C. V. C. Mendes, G. M. A. Almeida, M. L. Lyra, and F. A. B. F. de Moura, Phys. Rev. E **99**, 022117 (2019).
[24] A. R. C. Buarque and W. S. Dias, Phys. Rev. E **100**, 032106 (2019).
[25] M. A. Pires and S. M. Duarte Queirós, Sci. Rep. **11**, 4527 (2021).
[26] V. Kendon and B. Tregenna, Phys. Rev. A **67**, 042315 (2003).
[27] G. Alagic and A. Russell, Phys. Rev. A **72**, 062304 (2005).
[28] P. C. Richter, Phys. Rev. A **76**, 042306 (2007).
[29] V. Kendon, Math. Struct. Comp. Sci. **17**, 1169 (2007).
[30] C. Liu and N. Petulante, Phys. Rev. E **81**, 031113 (2010).
[31] S. E. Venegas-Andraca, Quant. Info. Proc. **11**, 1015 (2012).
[32] Y. Shikano, T. Wada, and J. Horikawa, Sci. Rep. **4**, 4427 (2014).
[33] C.-W. Lee, P. Kurzyński, and H. Nha, Phys. Rev. A **92**, 052336 (2015).
[34] J. P. Mendonça, F. A. B. F. de Moura, M. L. Lyra, and G. M. A. Almeida, Phys. Rev. A **101**, 062335 (2020).
[35] M. Maeda, H. Sasaki, E. Segawa, A. Suzuki, and K. Suzuki, Discrete Contin. Dyn. Syst. **38**, 3687 (2018).
[36] Y. Gerasimenko, B. Tarasinski, and C. W. J. Beenakker, Phys. Rev. A **93**, 022329 (2016).
[37] C. Navarrete-Benlloch, A. Pérez, and E. Roldán, Phys. Rev. A **75**, 062333 (2007).
[38] A. R. C. Buarque and W. S. Dias, Phys. Rev. A **101**, 023802 (2020).
[39] F. Lederer, G. I. Stegeman, D. N. Christodoulides, G. Assanto, M. Segev, and Y. Silberberg, Phys. Rep. **463**, 1 (2008).
[40] F. Dalfovo, S. Giorgini, L. P. Pitaevskii, and S. Stringari, Rev. Mod. Phys. **71**, 463 (1999).
[41] O. Morsch and M. Oberthaler, Rev. Mod. Phys. **78**, 179 (2006).
[42] X.-Y. Xu, Q.-Q. Wang, W.-W. Pan, K. Sun, J.-S. Xu, G. Chen, J.-S. Tang, M. Gong, Y.-J. Han, C.-F. Li, and G.-C. Guo, Phys. Rev. Lett. **120**, 260501 (2018).
[43] S. Dadras, A. Gresch, C. Groiseau, S. Wimberger, and G. S. Summy, Phys. Rev. Lett. **121**, 070402 (2018).
[44] B. Tregenna, W. Flanagan, R. Maile, and V. Kendon, New J. Phys. **5**, 83 (2003).
[45] T. Baumgratz, M. Cramer, and M. B. Plenio, Phys. Rev. Lett. **113**, 140401 (2014).
[46] Z. He, Z. Huang, L. Li, and H. Situ, Quant. Info. Proc. **16**, 271 (2017).

[47] Y. Yuan, Z. Hou, J.-F. Tang, A. Streltsov, G.-Y. Xiang, C.-F. Li, and G.-C. Guo, npj Quant. Info. **6**, 46 (2020).
[48] F. W. Strauch, Phys. Rev. A **73**, 054302 (2006).
[49] C. M. Chandrashekar, S. Banerjee, and R. Srikanth, Phys. Rev. A **81**, 062340 (2010).
[50] G. di Molfetta and F. Debbasch, J. Math. Phys. **53**, 123302 (2012).
[51] C. M. Chandrashekar, Sci. Rep. **3**, 2829 (2013).
[52] N. P. Kumar, R. Balu, R. Laflamme, and C. M. Chandrashekar, Phys. Rev. A **97**, 012116 (2018).
[53] G. Di Molfetta, L. Honter, B. B. Luo, T. Wada, and Y. Shikano, Quant. Stud.: Math. Found. **2**, 243 (2015).
[54] G. Di Molfetta, M. Brachet, and F. Debbasch, Phys. Rev. A **88**, 042301 (2013).
[55] H. Zhang, C.-X. Liu, X.-L. Qi, X. Dai, Z. Fang, and S.-C. Zhang, Nat. Phys. **5**, 438 (2009).
[56] C. W. Groth, M. Wimmer, A. R. Akhmerov, J. Tworzydło, and C. W. J. Beenakker, Phys. Rev. Lett. **103**, 196805 (2009).
[57] P. L. Knight, E. Roldán, and J. E. Sipe, Phys. Rev. A **68**, 020301 (2003).
[58] P. L. Knight, E. Roldán, and J. Sipe, Opt. Commun. **227**, 147 (2003).
[59] A. Schreiber, K. N. Cassemiro, V. Potoček, A. Gábris, P. J. Mosley,, E. Andersson, I. Jex, and C. Silberhorn, Phys. Rev. Lett. **104**, 050502 (2010).
[60] D. Pandey, N. Satapathy, M. S. Meena, and H. Ramachandran, Phys. Rev. A **84**, 042322 (2011).
[61] A. Crespi, R. Osellame, R. Ramponi, V. Giovannetti, R. Fazio, L. Sansoni, F. De Nicola, F. Sciarrino, and P. Mataloni, Nat. Photonics **7**, 322 (2013).